JMEPEG (1994) 3:551-559

Microstructural Effects on Formability of Type 304 Stainless Steel Sheet in Cylindrical Deep Drawing

J.-S. Chang and S.-S. Chou

Type 304 stainless steel 0.8-mm-thick sheets were deep drawn by a complex working process using a hot die and a cold punch. The working temperature ranged from 25 to 150 °C. In room-temperature performance, the sheet metal failed because of severe work hardening. As the temperature was raised, it also failed in shear instability due to its poor ductility and small rate of work hardening. The drawability was improved by nonhomogeneous deformation with a heated die and a cooled punch. This effect disappeared as the temperature was increased to 150 °C. The microstructures appearing under various working conditions were investigated, and effects on drawability of steel sheets are discussed.

Keywords:
austenitic stainless steel, microstructure, plastic deformation

1. Introduction

DEEP-DRAWING performance is generally improved by matching the plastic anisotropy of the material to the symmetry of the formation. Drawability is determined largely by the plastic anisotropy R of the material, with a high R value being desirable for good drawability. An analysis of the forces acting during the drawing process reveals that the strength of the forming cup wall increases with the R value of the sheet metal (Ref 1, 2). Good work-hardening characteristics, indicated by the value of the strain-hardening exponent n, are considered with plastic anisotropy as a combined criterion of good deep drawing quality. In the drawing process, however, materials possessing a large value of R have good drawability (Ref 3). Such a large value means decreased thickness strain and better thinning resistance.

The level of the forming limit increases as n and m increase (Ref 3, 4); n and m represent the strain hardening exponent and the strain-rate sensitivity in the constitutive equation, respectively (Ref 4). Hence, increase of both n and m achieves better formability. The coefficients n and m are functions of temperature (Ref 5, 6), generally, decreasing and increasing, respectively, with increasing temperature. Ordinarily, it is difficult to draw a type 304 stainless steel sheet into a cup at cold working due to its severe strain hardening, i.e., large value of n (Ref 3). Strain rate sensitivity m is correlated with temperature and martensitic transformation effects during deformation (Ref 7). In type 300 series stainless steels, martensitic transformation may be induced by plastic deformation far above the M_s temperature. The extent of transformation in type 304 stainless steel depends on both the deformation temperature and plastic strain (Ref 7-10), and decreases with increasing temperature at any given strains.

The ductility of type 304 stainless steel is greater at low temperatures than at elevated temperatures (Ref 7, 11), but the martensitic transformation is also greater at low temperature (Ref 12-14). The presence of martensite in the materials increases its hardness, being deleterious to overall formability (Ref 7). Bressanelli and Moskowitz (Ref 15) suggested that small ductility of type 304 stainless steel results from limited ductility of the martensite product causing decreased uniaxial ductility at low temperatures, which results in premature fracture. No effects of martensitic transformation are present at temperatures greater than 50 °C (Ref 12), but the ductility of type 304 stainless steel is also decreased. Improvement of the drawability at elevated temperatures is thus difficult.

In addition to phase transformation, twinning can occur in austenite during plastic deformation (Ref 16). Twinning stress increases with temperature and is directly related to the variation of stacking fault energy (SFE) (Ref 17). Hence, temperature strongly influences the deformation mode in austenite. Microstructure is also an important factor in influencing drawability (Ref 18). This work aims to investigate the effect of temperature on the drawability of type 304 stainless steel sheet by nonhomogeneous deformation with a hot die and a cooled punch in deep drawing. Discussed are the types of microstructures appearing in the sheet metal and their effects on its drawability.

2. Experimental Method

In the deep-drawing equipment of AMINO type, the die alignment is designed so that the die body is at the top half and the punch is at the bottom half. The die can be moved vertically by the AMINO system actuated with oil pressure. A 50-mm-diam. cylindrical punch, with its center drilled so that water can be pumped through, is fixed at the equipment body. Heaters and thermocouples were installed in the blank holder and the die in order to control their operating temperature. The chemical composition of type 304 stainless steel used in this experiment is: 0.06% C, 0.63% Si, 1.09% Mn, 0.03% P, 0.03% Cu, 0.01% S, 0.12% V, 8.63% Ni, 18.12% Cr, and the balance Fe. The disk-shaped sheet specimen was prepared from the 0.8-mm-thick stainless steel sheet. Experiments were performed at temperatures in the range of 25 to 150 °C, with and without a punch being cooled. Before the trial, the specimen was coated with a suitable amount of lubricant having high viscosity and placed between the blank holder and the die, heated to the desired temperature, and maintained at this value for 5 minutes. Then ice

J.-S. Chang and **S.-S. Chou**, Department of Materials Science and Engineering(22), National Cheng Kung University, Tainan, Taiwan, 70101, Republic of China.

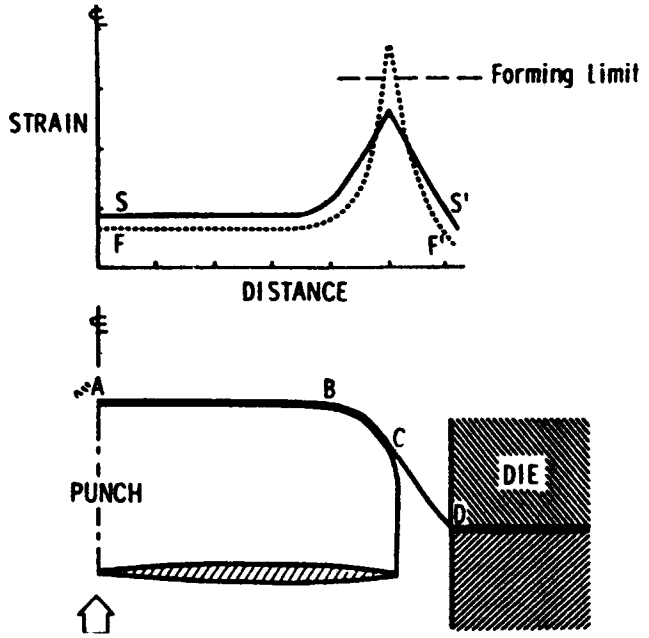

Fig. 1 Radial strain distribution for punch forming of a flat-ended cylindrical cup. From Ref 4. SS′ represents a successful part, and FF′ produces a neck. The largest strain position is taken for microstructural examination

water was pumped to flow through the punch. The specimen was then drawn into a cup by the flat-ended punch. The cups were drawn under varied operating temperatures, with or without ice water flowing through the punch. Cups produced under varied conditions were sliced with electric spark erosion into 3-mm-diam. disks for transmission electron microscope (TEM) examination and thickness measurement.

The disks for TEM examination were worn down equally on both surfaces to a thickness of 0.20 to 0.25 mm, then polished with a twin jet in a solution containing 10% perchloric acid and 90% acetic acid at 40 V DC. After jet polishing, these foils were rinsed with methanol to remove etchant that might have adsorbed on the foil surface. These thin foils were observed by a JEOL CX-200 transmission electron microscope operated at 200 kV accelerating voltage. To identify crystallographic features including ε-phase, α′-martensite, and deformation structures, representative areas were examined with a selected-area diffraction (SAD) technique.

3. Experimental Results

A cylindrical cup formed successfully to the full depth by a warm deep-drawing performance associated with a cooled punch, but full depth was not attained when the punch had not been cooled during the warm- or cold-working performance. Experimental results, listed in Table 1, indicate that successful cup forming occurs with warm, nonhomogeneous plastic deformation between 50 and 125 °C. Besides difficult forming at room temperature, forming successfully at temperatures up to 150 °C is difficult even though cooling in the punch is still maintained. It fails under warm working at approximately 50 to 125 °C without cooling also in the punch.

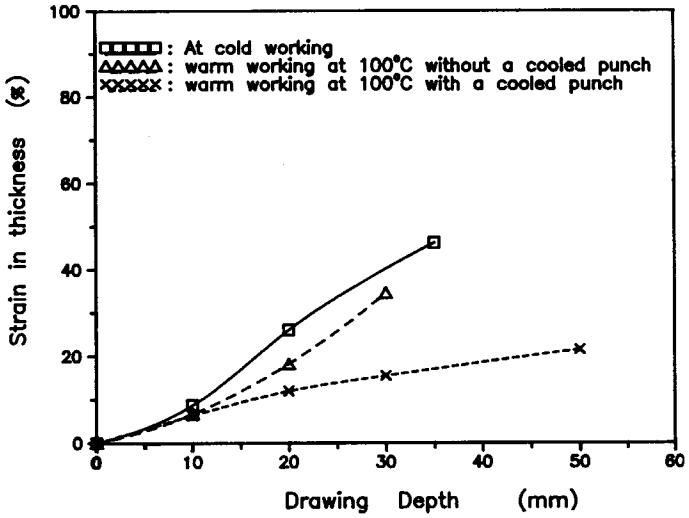

Fig. 2 Variation of the shear straining rate with the incremental drawing depth in cylindrical deep drawing

Table 1 Forming height of deep-drawn cups

Temperature, °C	Punch cooled, height, mm	Not cooled, height, mm
25	...	34.50
50	50.20	31.30
75	50.45	...
100	50.60	30.70
125	49.80	...
150	22.25	...

3.1 *Rate of Shear Straining*

In punch forming of a cylindrical cup with a flat end, the breakdown point generally occurred at the punch shoulder portion. As a punch radius acted as a strain and stress concentrator, the largest strain location in Fig. 1 was the source of foil specimens for TEM observation and thickness measurement. When specimens were deep drawn at a fixed condition to varied depths incrementally, the thickness strains were calculated as $(S_o - S)/S$. S_o and S represent the original thickness of the specimen and the current thickness of the breakdown point, respectively, and are plotted with corresponding drawing depth in Fig. 2. The greatest ductility and a much increased rate of shear straining occur at room temperature. Warm working at a single temperature, 100 °C, yields an intermediate rate of shear straining and poor drawability whereas warm working with a cooled punch produces the smallest rate of shear straining.

3.2 *Microstructure of Cold Working*

Before microstructural examination of the deep-drawn cup, we verified that undesired microstructures, such as martensite and mechanical twins that may be generated during the abrasive process or specimen preparation, were not induced. Only dislocation and stacking faults were observed in the thin foil of the original material. From tests at room temperature, the microstructure is observed as strain-induced martensite that forms by a process requiring dislocations at a large concentra-

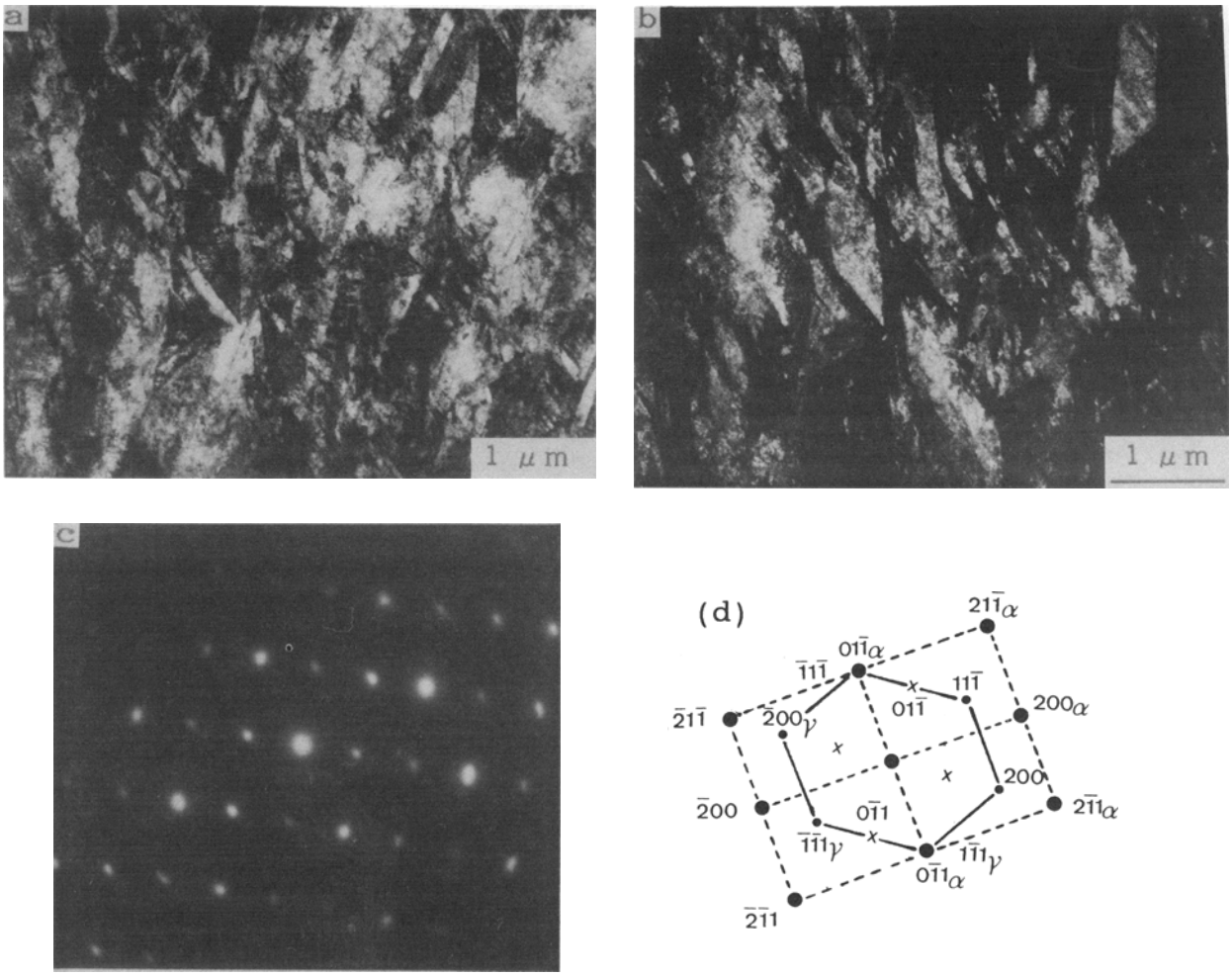

Fig. 3 Electron micrograph of the break-down point deformed at 25 °C. (a) Bright field image of dense martensite product. (b) Dark field image on $(01\bar{1})$ reflection. (c) Diffraction pattern and (d) its identification

tion. The martensite appears as a densely blocky structure and has poor drawability. The presence of martensite induced by plastic strain may cause an increased hardness and localized instability; then fracture occurs. Illustrated in Fig. 3 are α'-martensite and its dark field image of a $(01\bar{1})$ diffraction spot reflection. Much more dense dislocations accumulated about the martensite, which were caused by plastic deformation.

3.3 *Warm Working in Single Temperature*

The performance at elevated temperature (100 °C) failed when the punch was not cooled. The microstructure at the breakdown point was observed as a twin band combined with parallel dislocation tangles, as shown in Fig. 4. The edge-on twin band and its dark field image on the $(11\bar{1})$ reflection are shown in Fig. 4(a) and (b), respectively. The parallel dislocation tangles were observed only when the foil tilted some degrees with respect to the $(11\bar{1})$ twin band, as shown in Fig. 4(d). Thus, twin band and parallel dislocation tangles are located in the different plane; cross slip occurred. The intersection number of shear bands was decreased at elevated temperatures, and the twin band generated by the shear stress was wider.

3.4 *Warm Working with a Cooled Punch*

When the punch was cooled during warm working, microstructure at the breakdown point appeared as the intersection of deformation twins and slip bands at 50 °C, as shown in Fig. 5. Figures 5(b-e) also show diffraction patterns and dark-field images of the twins and ε slip bands, respectively. The deformation twins associated with conjugate twinning at 100 °C are shown in Fig. 6(a). Figure 6(b) is the diffraction pattern of two twinning variants, and Fig. 6(c) and (d) show the dark field reflections of two conjugate twins, respectively. The twin-twin intersections combined with twin-slip intersections both appear at 75 °C (not shown). Distinct temperatures acting on both sides of the specimen cause slip systems to become more active on the two sides during deep drawing. These two main systems meet at the mid thickness of the cup wall and impinge each other. Finally, they form as the intersection of twins and slip bands.

3.5 *Warm Working at Higher Temperature*

When the temperature was increased to 150 °C and the punch still cooled with ice water, twin bundles with dislocations accumulated at their boundaries, as shown in Fig. 7. Mi-

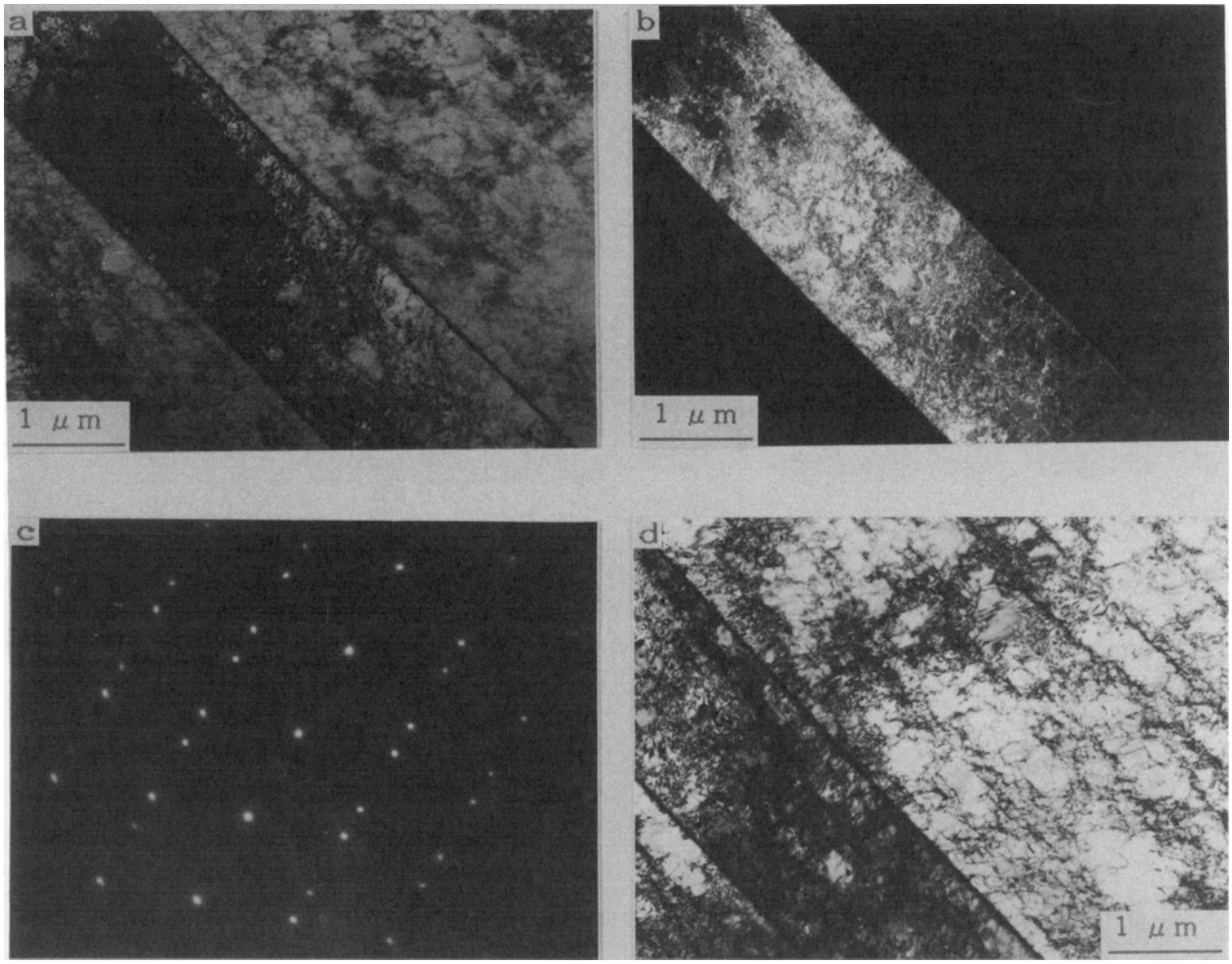

Fig. 4 Electron micrograph of the break-down point deformed at 100 °C without cooling in the punch. (a) Bright field image of parallel-edged twin band. (b) Dark field image on $(11\bar{1})$ twin spot reflection. (c) Diffraction pattern of twin. (d) Declined a few degrees to the edged-on twin band (a) showing the parallel dislocation tangles

crostructures of these types cause brittle failure, as shown by a fractograph in Fig. 7(d). At present. the causes of failure are considered to be insufficient cooling with ice water and poor ductility of materials at this high temperature. To obtain better drawability of type 304 stainless steel, a suitable performance temperature and an appropriate temperature difference must exist concurrently between both sides of the deep-drawn specimen. If not, the strength of internal grains becomes decreased as the twinning bundles act as obstacles for motion of dislocations that accumulate at their boundaries.

4. Discussion

At room temperature, the drawability of a type 304 stainless steel sheet is poor because of its strongly strain hardening character and greater production of thickness strain during plastic deformation. As the martensite induced by plastic strain increases, the accumulation of dislocations enhances work hardening of a metastable austenitic stainless steel. α'-martensite behaves as a hardening body and an accelerator of storage of dislocations in the austenitic phase (Ref 19). It also acts as an obstacle for slip, resulting in increased dislocation density in the austenitic phase. Therefore, martensite transformation becomes saturated sooner, and a rapidly decreased rate of work hardening yields premature local plastic instability (Ref 12). The fact that type 304 stainless steel draws poorly under cold working is thus explained.

At room temperature, more extensive martensite induced by strain causes both flow stress and the rate of strain hardening to increase, and leads to poor drawability. An optimum rate of martensite formation or work hardening is required for extensive formability in unstable austenitic steels. The rate of transformation must suffice to prevent onset of necking, but must not be excessive so as to induce early fracture in the less ductile martensite (Ref 15, 20). When the material is heated during deep drawing, softening occurs due to small strain of the γ-phase and decreased α'-phase. The increased temperature during deep drawing suffices to suppress the γ - α' transformation substantially. Both rates of strain hardening (Ref 7) and martensitic transformation (Ref 12) of type 304 stainless steel decrease with increasing temperature. The drawability remains poor due to its low ductility at elevated temperatures.

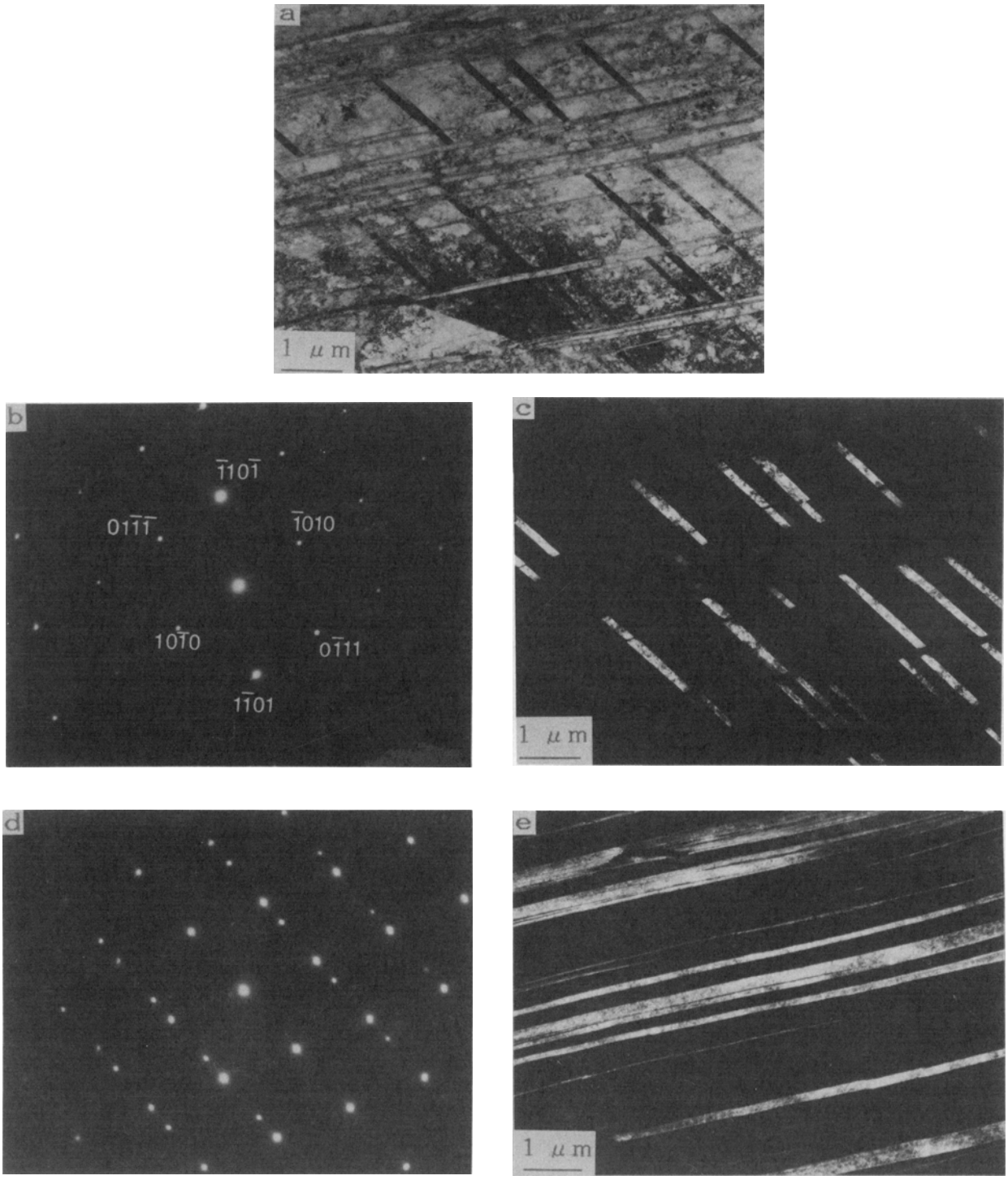

Fig. 5 Electron micrograph of the break-down point deformed at 50 °C with a cooled punch. (a) Bright field image of twin and slip band intersections. (b) Diffraction pattern of cph slip band and (c) its dark field image on ($1\bar{1}01$) reflection. (d) Diffraction pattern of twin and (e) its dark field image on (111) twin spot reflection

The mode of strain-induced martensite is favored near the Md temperature (Ref 21), the temperature above which deformation stresses cannot initiate the martensitic transformation. At temperatures above Md, yielding occurs entirely by slip of the austenite. Homogeneous glide in a single slip system occurs dominantly at 100 °C when the punch is not cooled; dislocation pile-up groups may propagate into a twin band within a brief period. Because the accumulated stress is large enough and cannot be relieved, the internal strength of the grains is too weak to resist external stress; hence, shear occurs homogeneously along the direction of the applied stress leading to failure at the highly stressed point. As illustrated in Fig. 4, twin band

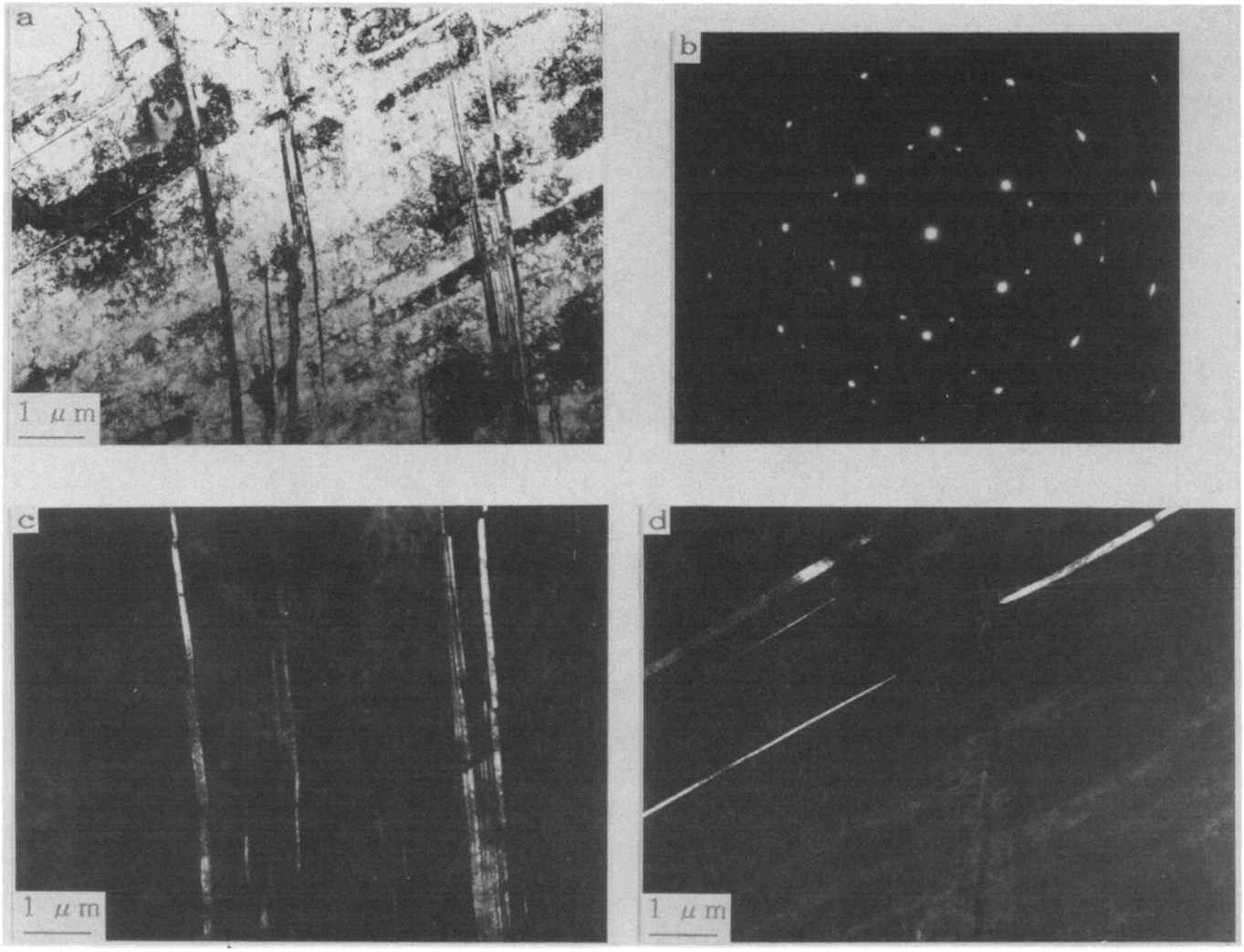

Fig. 6 Electron micrograph of the break-down point deformed at 100 °C with a cooled punch. (a) Bright field image of two twin intersections. (b) Diffraction pattern of two twin variants. (c) and (d) Dark field images on conjugate twinning reflections

with a large width possesses a high stored energy (Ref 22) and is less stable. The two edges of the twin band must coincide with the direction of shear stress. Because these two edges and the parallel dislocation tangles having weakly secondary slip are located at different planes, cross slip occurs under applied stresses. The role of cross slip during this homogeneously plastic deformation promotes the propagation of twin band and shear instability.

Internal stresses due to accumulated dislocation or interactions of forest dislocations can be relaxed by slipping on the secondary systems (Ref 22, 23). We attempted to activate these secondary systems by cooling the punch while the die is heated. Varied straining due to the temperature difference on either side of the specimen caused slip on the secondary systems, and these dislocations interacted with primary dislocations to form stable Lomer-Cottrell dislocations that relaxed internal stresses continually. If the punch was cooled and the die side heated to a certain temperature between 50 and 100 °C, twin-slip and twin-twin intersections appeared at the point of breakdown. The flow and yield stresses and the strain of type 304 stainless steel decrease sensitively with increasing temperature, as shown in Fig. 8 and 9. The specimen deforms in a nonhomogeneous way due to different temperatures on the two sides of the specimen. Nonhomogeneous slipping, depicted in Fig. 10, illustrates the comparison with the same and distinct shear strainings on the two sides of the specimen. The distinct strainings on both sides deform under varied flow stresses so that effective slips are generated in more than one slip system and impinge each other. For the drawing axial tension, the Schmid factor expressed by $m = \sigma_a/\sigma_s = \text{Cos}\lambda\text{Cos}\varphi$ indicates that m is the function of the applied axial tensile stress, σ_a, the shear stress in the slip direction, σs, the angle between the stress axis and the slip plane normal, and the angle between the stress axis and the slip direction. Therefore, the slip direction depends on the flow stress acted on either side of the specimen. It is possible to conclude the experimental results so that the number of active slip systems is higher for two-temperature deformation than for one-temperature, and that the amount of slipping on each slip system is more uniformly distributed in the former. Therefore, the slip lines or bands of the first slip system act as obstacles to the secondary one and interact with each other to relieve stress concentration. Thus at 50 °C with the cooled

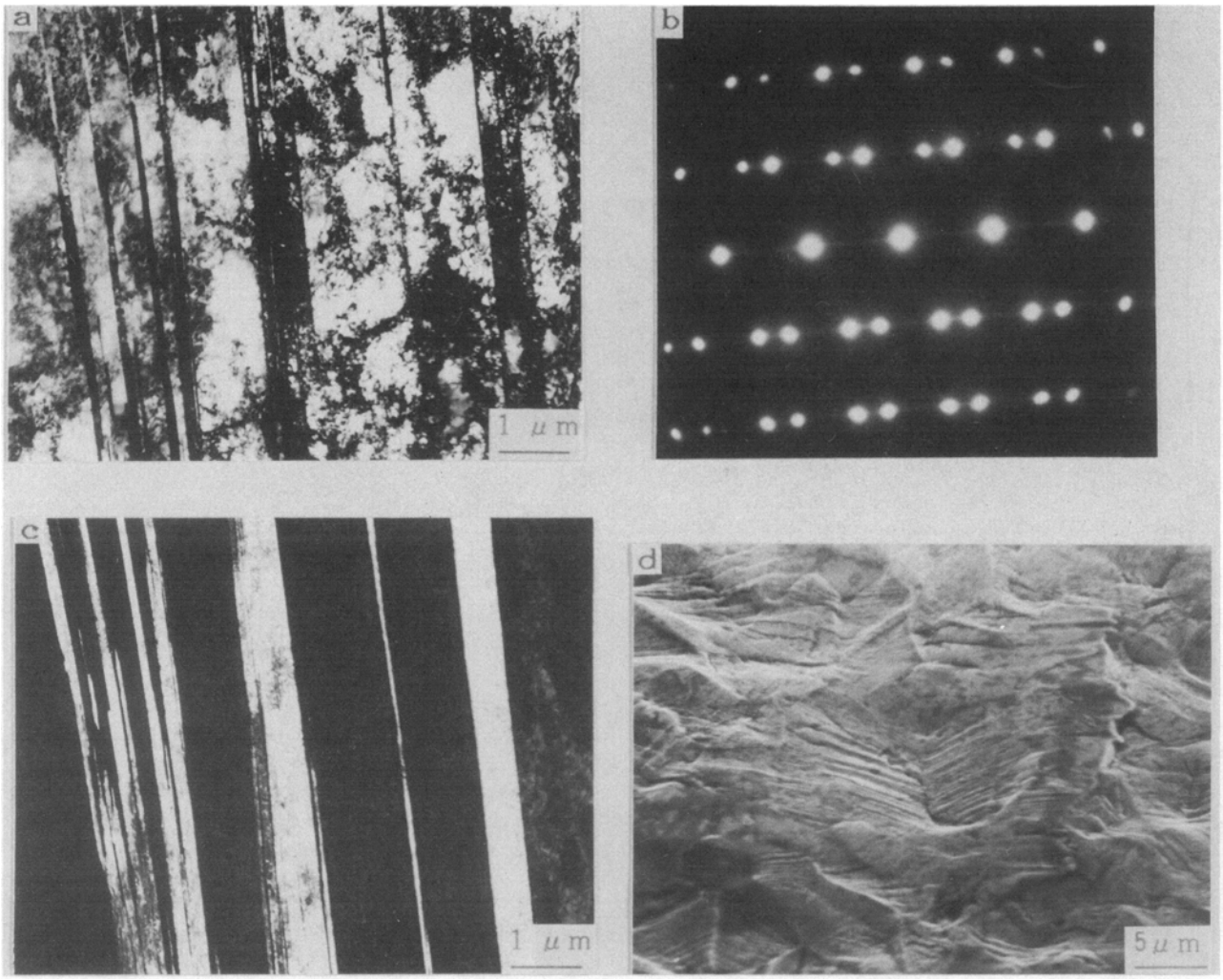

Fig. 7 Electron micrograph of the break-down point deformed at 150 °C with a cooled punch. (a) Bright field image of twin bundles associated with high density dislocations. (b) Diffraction pattern of twin and (c) its dark field image on (111) twin spot reflection. (d) Fractography shows a brittle cleavage

punch, the primary slip dislocation intersecting a secondary slip dislocation produces Lomer-Cottrell dislocations to make it the twin source of the most favorable type in the crystal, described as the dislocation mode (Ref 24) for twinning in the low SFE alloys. Twinning occurs on the primary system and slip bands on the secondary system, which intersect with each other at the mid thickness. The shear offsets created at intersections also exhaust some strain energy to transfer the shear strain. Then the grains are strong enough to resist shear instability.

In a polycrystalline metal, a greater difference of temperature between the two sides generates a larger gradient of flow stress in grains as the temperature is increased to 100 °C, and accumulated stresses are relieved by twin-twin intersections. Accumulation of dislocations on the primary slip plane can act as twinning sources on one side when they are intersected by the secondary slip dislocations. A similar accumulation of dislocations produced by the secondary slip dislocations are sources of twins on the other side. Twinning on one side occurs heterogeneously from that on the other side, and twinning deformations also occur on twinning planes separate from each other in the conjugate relation. Thus, in conditions under which the internal stress is the same on both systems, conjugate twin-twin intersections are formed and occur on both conjugate planes throughout the crystal. Both the interactions of two twins and twin-slip provide a remarkable reduction in their widths and have a smaller stored energy (Ref 22) so that they are more stable.

When the die is heated to 150 °C and the punch is cooled by ice water, unidirectionally discrete twinning bundles are observed. Slipping in secondary directions cannot be maintained at this temperature, as the temperature gradient on the two sides is decreased so as not to preserve effectively slipping in the secondary system. Only twinning and accumulation of dislocations occurred in the primary slip system. From the dislocation theory of fracture (Ref 25, 26), the effect of twins plays an important role, modifying the dislocation path and acting as barriers, and cleavage fracture is nucleated. Once nucleation occurs, a cleavage crack causes repeated twinning, and the resulting retardation of the crack is unable to stop its advance. In the case of twinned samples, fracture occurs as a result of virtually pull-

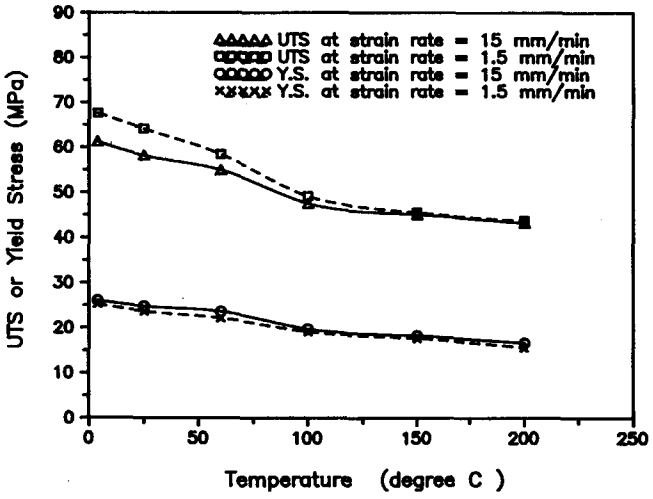

Fig. 8 Dependence of ultimate tensile strength (UTS) and yield stress of type 304 stainless steel on temperature

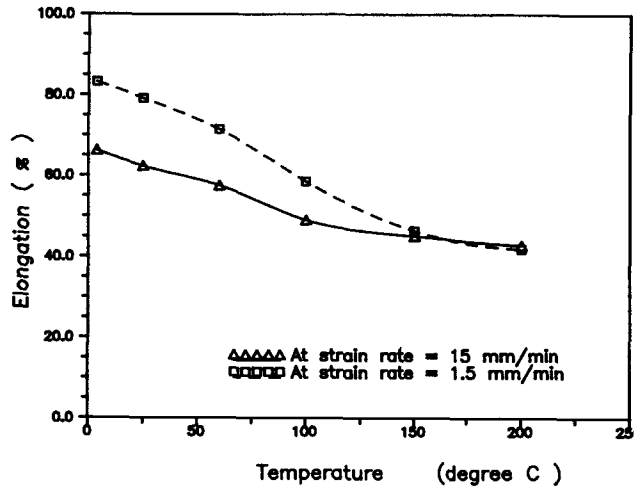

Fig. 9 Dependence of the elongation of type 304 stainless steel on temperature

ing the atomic planes apart when the theoretical strength is exceeded.

5. Conclusion

Type 304 stainless steel disk-shaped sheet was used for a deep-drawing test. The cylindrical cup products subjected to microstructural examination with a transmission electron microscope are described as follows:

- At room temperature, the microstructure of densely blocky martensite appears at the breakdown point. Increased thickness strain that occurs at low temperatures produces strain-induced martensite that has smaller ductility leading to localized instability and break at the part of a cup wall at which stress is concentrated.
- When the temperature is increased to 100 °C and the punch is not cooled, homogeneous deformation occurs by twinning and gliding in a single slip system. A widened twin band associates with parallel dislocation tangles acting as a cross slip. This effect may cause the rapid rate of shear straining.
- In conditions with a cooled punch and a heated die, twin-slip and/or twin-twin intersections are generated at the highly stressed point. The rate of shear straining is greatly decreased, and improved effects on deep-drawing performance are generated.
- As the temperature is raised to 150 °C, twin bundles associated with dislocations accumulated against their boundaries appeared, causing brittle fracture to occur. A limit of performance temperature may exist in warm deep drawing of type 304 stainless steel sheets.

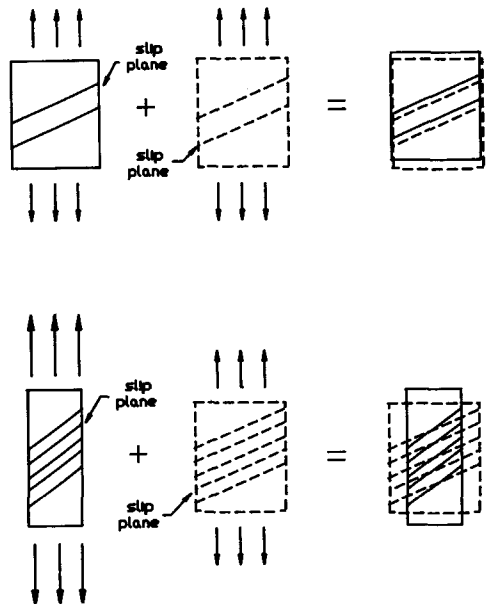

Fig. 10 Deformation behavior on each side of the sheet specimen. (a) Same straining on both sides produces a homogeneous deformation. (b) Combination of different strainings on both sides generates a heterogeneous deformation. The glide dislocations distribute more uniformly on slip systems of (b) than of (a)

Acknowledgment

The authors are grateful to Metal Industry Development Center for supplying equipment during this deep drawing study. This study is sponsored by the National Science Council of R.O.C.

References

1. W.T. Lankford, S.C. Snyder, and J.A. Bauscher, *Trans. ASM*, Vol 42, 1950, p 1197-1232
2. R.L. Whiteley, *Trans. ASM*, Vol 52, 1960, p 154-169
3. Z. Marciniak and K. Kuczynski, *Int. J. Mech. Sci.*, Vol 9, 1967, p 609-620
4. A.K. Ghosh, *J. Eng. Mater. Technol. (Trans. ASME)*, 1977, p 264-274

5. J. Klepaczko, *Int. J. Mech. Sci.*, Vol 10, 1968, p 297-313
6. J.R. Klepaczko, *J. Mech. Work. Technol.*, Vol 15, 1987, p 143-165
7. G.L. Huang, D.K. Matlock, and G. Krauss, *Metall. Trans. A*, Vol 20, 1989, p 1239-1246
8. A.K. Ghosh, *Acta Metall.*, Vol 25, 1977, p 1413-1424
9. A.K. Ghosh, *Metall. Trans. A*, Vol 8, 1977, p 1221-1232
10. A.K. Ghosh and R.A. Ayres, *Metall. Trans. A*, Vol 7, 1976, p 1589-1591
11. T. Suzuki, H. Kojima, K. Suzuki, T. Hashimoto, and M. Ichihara, *Acta Metall.*, Vol 25, 1977, p 1151-1162
12. S.S. Hecker, M.G. Stout, K.P. Staudhammer, and J.L. Smith, *Metall. Trans. A*, Vol 13, 1982, p 619-626
13. T. Angel, *J. Iron Steel Inst. (London)*, Vol 177, 1954, p 165-174
14. G.B. Olson, *Deformation Process and Structure*, G. Krauss, Ed., ASM, 1984, p 391-424
15. J.P. Bressanelli and A. Moskowitz, *Trans. ASM*, Vol 59, 1966, p 223-239
16. M. Blicharski and S. Gorczyca, *Met. Sci.*, July 1978, p 303-311
17. J.A. Venables, *J. Phys. Chem. Solid*, Vol 25, 1964, p 693-715
18. F. Ronde-Oustau and B. Baudelet, *Acta Metall.*, Vol 25, 1977, p 1523-1529
19. T. Narutani, *Mater. Trans., JIM*, Vol 30 (No. 1), 1989, p 33-45
20. P.C. Maxwell, A. Goldberg, and J.C. Shyne, *Metall. Trans.*, Vol 5, 1974, p 1319-1324
21. D. Bhandarker, V.F. Zackay, and E.R. Parker, *Metall. Trans.*, Vol 3, 1972, p 2619-2631
22. N. Hansen and D. Kuhlmann-Wilsdorf, *Mater. Sci. Eng.*, Vol 81, 1986, p 141-161
23. D. Kuhlmann-Wilsdorf and N.R. Comins, *Mater. Sci. Eng.*, Vol 60, 1983, p 8-24
24. J.B. Cohen and J. Weertman, *Acta Metall.*, Vol 11, 1963, p 996-998
25. W.D. Biggs and P.L. Pratt, *Acta Metall.*, Vol 6, 1958, p 694-703
26. P.L. Mangonon, Jr. and G. Thomas, *Metall. Trans.*, Vol 1, 1970, p 1587-1594